

Supplementary information

Tuning the solubility of boron nitride nanosheets in organic solvents by using block copolymer as a “Janus” modifier

Yi-Tao Liu^a, Xu-Ming Xie^{a} and Xiong-Ying Ye^b*

^a Advanced Materials Laboratory, Department of Chemical Engineering, Tsinghua University,

Beijing 100084, China

^b Department of Precision Instruments and Mechanology, Tsinghua University, Beijing 100084, China

* Corresponding author.

E-mail address: xxm-dce@mail.tsinghua.edu.cn

Contents

- S1 Experimental details
 - S1.1 Raw materials
 - S1.2 Exfoliation of natural BN powder
 - S1.3 Modification of BNNSs with P(S-*b*-MMA) by π - π stacking
 - S1.4 Modification of BNNSs with P(S-*b*-MMA) by coordination
 - S1.5 Nanocomposites preparation
- S2 Equipment and characterization techniques
- S3 Characterization of P(S-*b*-MMA)
- S4 TGA measurement on SM-*pi*-BNNSs
- S5 FTIR spectra of BNNSs, SM-*pi*-BNNSs and SM-*co*-BNNSs
- S6 Raman spectra of BNNSs, SM-*pi*-BNNSs and SM-*co*-BNNSs
- S7 Characterization of SM-*pi*-BNNSs solubility
- S8 HRTEM images of SM-*pi*-BNNSs and SM-*co*-BNNSs
- S9 Digital images of nanocomposite films
- S10 Representative S-S curves of nanocomposite films
- S11 SEM images of nanocomposite films

S1. Experimental details

S1.1 Raw materials

h-BN powder was purchased from Sigma-Aldrich. P(S-*b*-MMA) ($M_n = 160\ 000$; PS = 50 %; PDI = 1.09) was purchased from Polymer Source, and its structural formula is shown below. PS ($M_w = 330\ 000$) was purchased from Beijing Yanshan Petrochemical Co., Ltd., Sinopec. PMMA ($M_w = 350\ 000$) was purchased from Alfa Aesar. The other chemical reagents employed in this work were purchased from Beijing Chemical Works, and used as received.

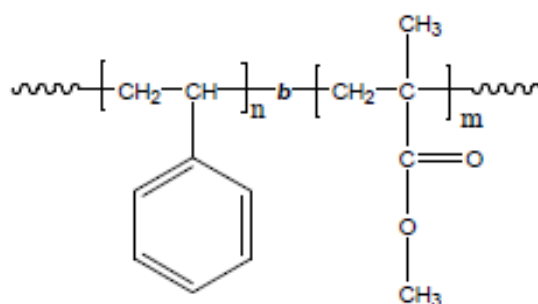


Fig.S1. Structural formula of P(S-*b*-MMA).

S1.2 Exfoliation of natural BN powder

The details for exfoliating h-BN powder into BNNSs could be found elsewhere [1]. Briefly, h-BN powder was added to NMP at an initial concentration of $3\ \text{mg mL}^{-1}$, and subjected to sonication at 70 W for 24 h. The obtained slurry was centrifuged at 1 500 rpm for 45 min, and the top 1/3 supernatant was collected, yielding a solution of single- and few-layer BNNSs. The supernatant was then filtered with a polytetrafluoroethylene (PTFE) filter membrane. The entrapped solid was collected, dried in vacuum, and redispersed in a series of organic solvents as controls.

[1] J. N. Coleman, M. Lotya, A. O'Neill, S. D. Bergin, P. J. King, U. Khan, K. Young, A. Gaucher, S. De, R. J. Smith, I. V. Shvets, S. K. Arora, G. Stanton, H.-Y. Kim, K. Lee, G. T. Kim, G. S. Duesberg, T. Hallam,

J. J. Boland, J. J. Wang, J. F. Donegan, J. C. Grunlan, G. Moriarty, A. Shmeliov, R. J. Nicholls, J. M. Perkins, E. M. Grieverson, K. Theuwissen, D. W. McComb, P. D. Nellist and V. Nicolosi, *Science*, 2011, **331**, 568.

*S1.3 Modification of BNNSs with P(S-*b*-MMA) by π - π stacking*

It is known that the hexagonal π -electron system of aromatic rings is isomorphic to that of BNNSs. Therefore, rational π - π stacking is expected to exist between them. In a typical run, h-BN powder was predispersed in NMP by sonication at 70 W for 4 h. Then excess P(S-*b*-MMA) was added, and the mixture was sonicated at 70 W for 20 h such that the P(S-*b*-MMA) chains could sufficiently adjust their conformation and be adsorbed on the exfoliated BNNSs by π - π stacking to stabilize them. Note that a relatively long time was needed to realize this conformational adjustment. The obtained slurry was centrifuged at 1 500 rpm for 45 min. The top 1/3 supernatant was collected, and then filtered with a PTFE filter membrane. The entrapped solid (SM-*pi*-BNNSs) was collected, rinsed with chloroform several times, dried in vacuum, and redispersed in a series of organic solvents.

*S1.4 Modification of BNNSs with P(S-*b*-MMA) by coordination*

In a typical run, h-BN powder was sonicated in NMP at 70 W for 24 h. The obtained slurry was centrifuged at 1 500 rpm for 45 min, and the top 1/3 supernatant was collected. Then P(S-*b*-MMA) and a small quantity of copper salt were added, and the mixed solution was kept at 80 °C under gentle stirring for 12 h. The wt ratio of P(S-*b*-MMA) to BNNSs was ~35 : 65, the same as that in SM-*pi*-BNNSs as determined by TGA (Fig. S4). Note that adding a copper salt alone to the BNNS solution resulted in immediate precipitation, due to the direct cross-linking of the nanosheets. Such cross-linking largely impairs the solution-phase processability of BNNSs. When P(S-*b*-MMA) was present, however, the polymer chains could effectively isolate the nanosheets by ion coordination. The whole system could be stable for days

without obvious precipitation. On the other hand, when a copper slat was added BNNSs tended to be bonded with P(S-*b*-MMA) by coordination, since it was a stronger interaction than π - π stacking. Moreover, coordination did not need the complex conformational adjustment required by π - π stacking. Once the surface of BNNSs was occupied by the P(S-*b*-MMA) chains by coordination, there was little room for further π - π stacking due to the steric hindrance. After filtration, the entrapped solid (SM-*co*-BNNSs) was collected, rinsed with chloroform several times, dried in vacuum, and redispersed in a series of organic solvents.

S1.5 Nanocomposites preparation

To prepare the PMMA-matrix nanocomposites, BNNSs and SM-*pi*-BNNSs were added to PMMA/DMF solutions separately at a filler content of 2 wt %, and stirred until being dissolved. The mixed solutions were poured in Teflon Petri dishes, and subjected to vacuum deposition at 80 °C until the weight equilibrated. To prepare the PS-matrix nanocomposites, BNNSs and SM-*co*-BNNSs were added to PS/DMF solutions separately at a filler content of 2 wt %, and stirred until being dissolved. The mixed solutions were poured in Teflon Petri dishes, and subjected to vacuum deposition at 80 °C until the weight equilibrated.

S2. Equipment and characterization techniques

UV-vis spectra were recorded by a Pgeneral TU-1810 twin-beam spectrophotometer from 200 to 900 nm.

Raman spectra were recorded by a Renishaw RM2000 spectrometer with 514 nm laser excitation.

FTIR spectra were recorded by a Nicolet 560 spectrometer.

TGA was recorded by a Shimadzu DTG-60 from ambient temperature to 800 °C with a heating rate of 20 °C min⁻¹ in air (40 mL min⁻¹).

DSC was recorded by a Shimadzu DSC-60 from ambient temperature to 170 °C with a heating rate of 10 °C min⁻¹ in nitrogen (40 mL min⁻¹).

TEM was performed by a Hitachi H7700 operated at an accelerating voltage of 100 kV.

HRTEM was performed by a JEOL JEM-2010 operated at an accelerating voltage of 120 kV.

AFM was performed by a Shimadzu SPM-9500 in the tapping mode.

SEM was performed by a Tescan VEGA3 operated at an accelerating voltage of 10 kV.

S3. Characterization of P(S-*b*-MMA)

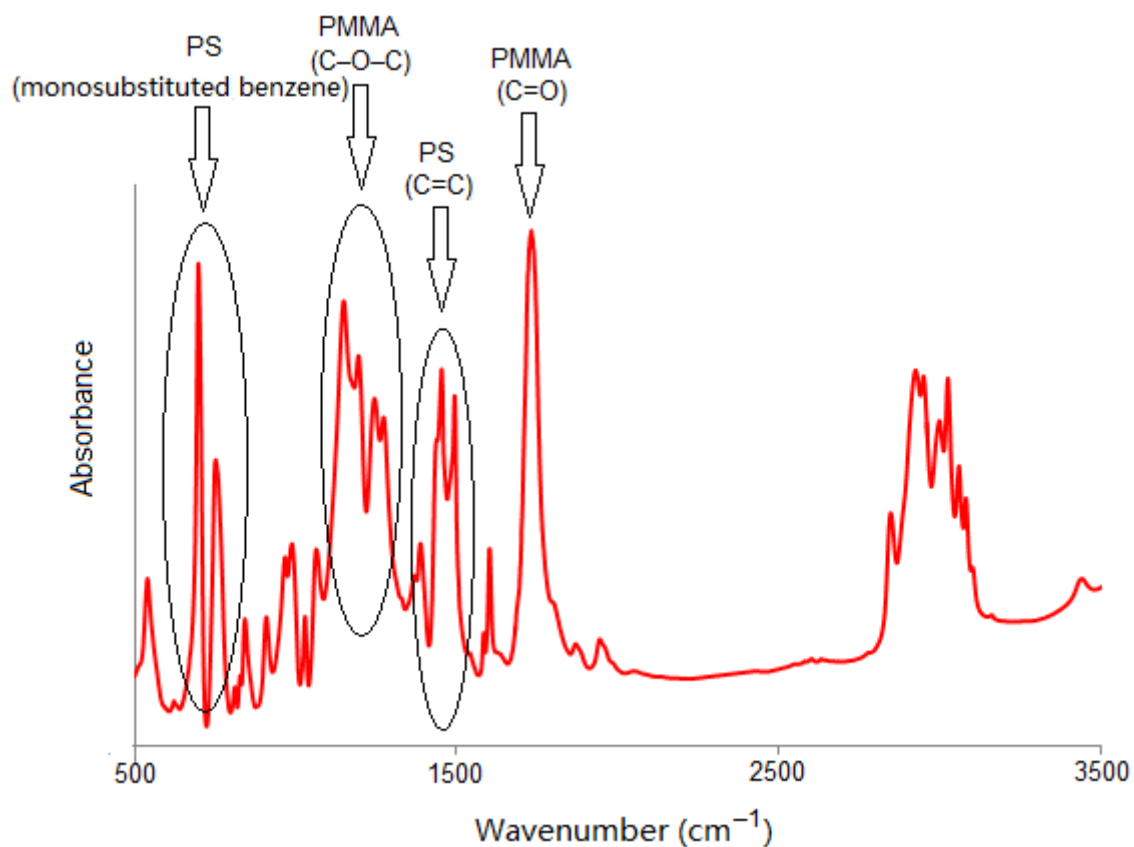


Fig.S2. FTIR spectrum of P(S-*b*-MMA).

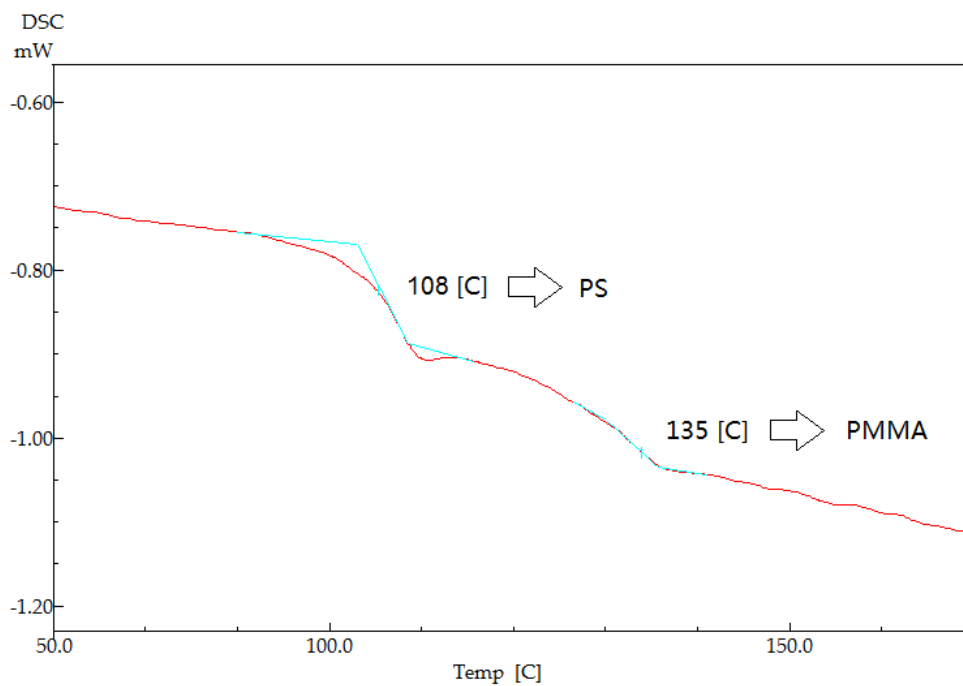


Fig.S3. DSC curve of P(S-*b*-MMA) giving the glass transition temperatures of the PS block (108 °C) and the PMMA block (135 °C).

S4. TGA measurement on SM-*pi*-BNNs

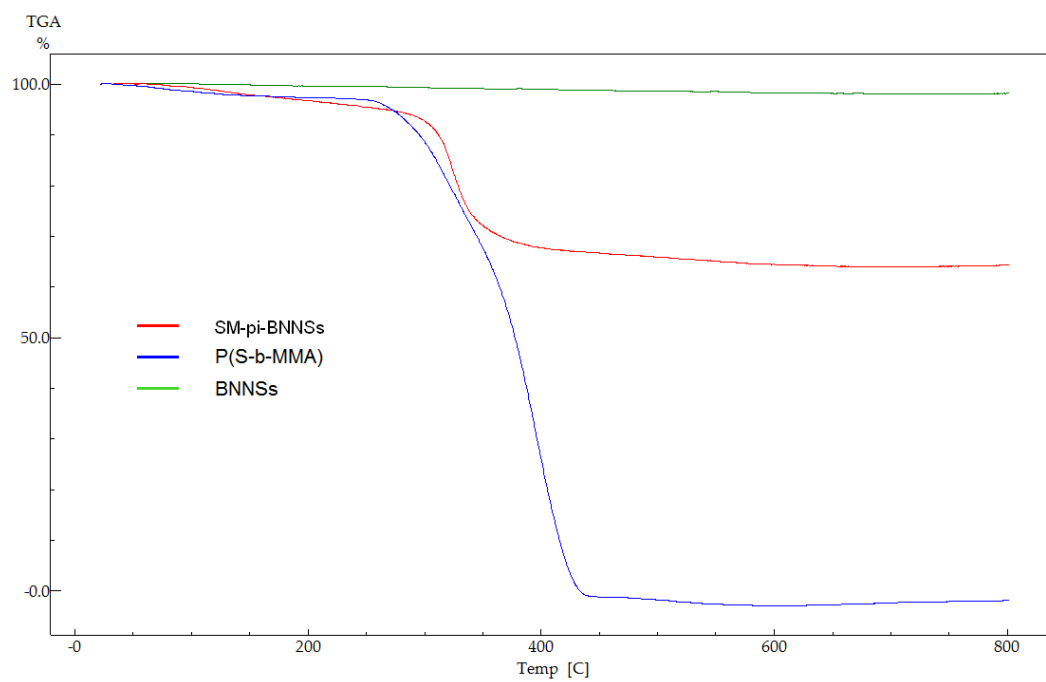


Fig. S4. TGA curves of BNNs, P(S-*b*-MMA) and SM-*pi*-BNNs showing that the content of P(S-*b*-MMA) in SM-*pi*-BNNs is ~35 wt %.

S5. FTIR spectra of BNNSs, SM-*pi*-BNNSs and SM-*co*-BNNSs

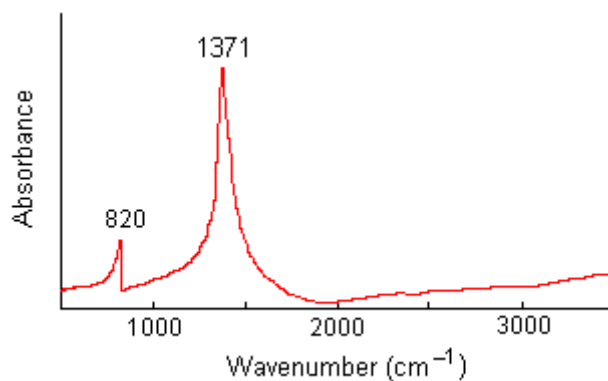


Fig.S5. FTIR spectrum of BNNSs, where the characteristic peaks at 820 and 1371 cm⁻¹ correspond to the shearing B–N–B binding mode and the stretching of the B–N bonds, respectively [1,2].

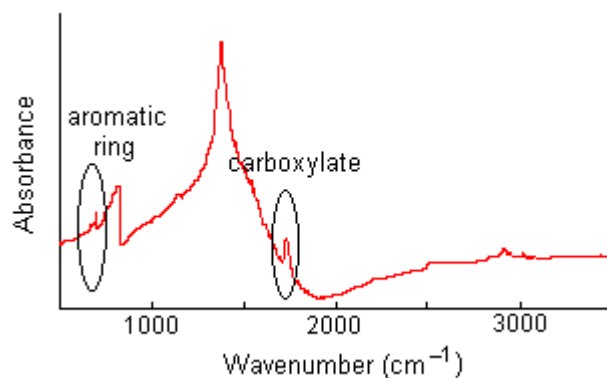


Fig.S6. FTIR spectrum of SM-*pi*-BNNSs, where the characteristic peaks at 696 and 750 cm⁻¹ (aromatic ring) and at 1728 cm⁻¹ (carboxylate) indicate the presence of P(S-*b*-MMA) on BNNSs [3,4].

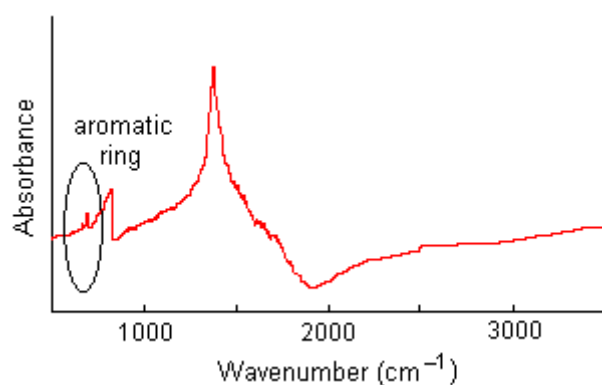


Fig.S7. FTIR spectrum of SM-*co*-BNNSs, where the characteristic peaks at 696 and 750 cm⁻¹ (aromatic ring) indicate the presence of P(S-*b*-MMA) on BNNSs, while the absence of the characteristic peak at 1728 cm⁻¹ indicates the successful coordination between the carboxylate groups and BNNSs [5].

- [1] C. Zhi, Y. Bando, C. Tang, H. Kuwahara and D. Golberg, *Adv. Mater.*, 2009, **21**, 2889.
- [2] S.-Y. Xie, W. Wang, K. A. S. Fernando, X. Wang, Y. Lin and Y.-P. Sun, *Chem. Commun.*, 2005, 3670.
- [3] Y.-T. Liu, W. Zhao, Z.-Y. Huang, Y.-F. Gao, X.-M. Xie, X.-H. Wang and X.-Y. Ye, *Carbon*, 2006, **44**, 1581.
- [4] Y.-T. Liu, X.-M. Xie and X.-Y. Ye, *Carbon*, 2011, **49**, 3529.
- [5] C. S. Kim and S. M. Oh, *Electrochim. Acta*, 2000, **45**, 2101.

S6. Raman spectra of BNNSs, SM-*pi*-BNNSs and SM-*co*-BNNSs

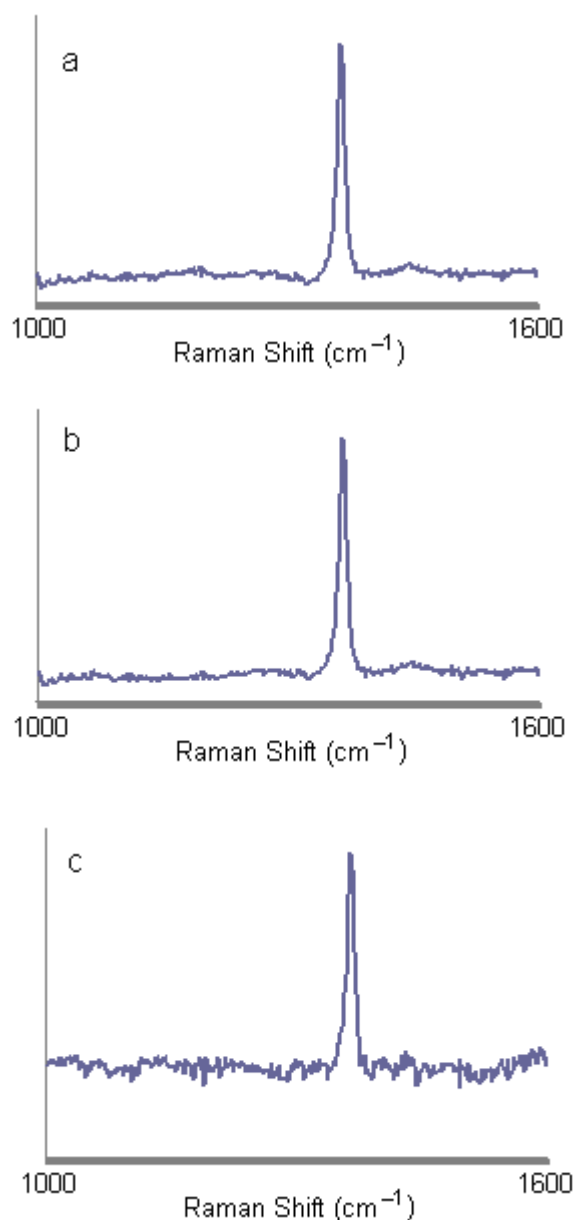


Fig. S8. Raman spectra of (a) BNNSs, (b) SM-*pi*-BNNSs and (c) SM-*co*-BNNSs, where the characteristic peak at $\sim 1365\text{ cm}^{-1}$ is attributed to the B-N high-frequency vibrational mode (E_{2g}) within the BN layers [1]. Note that there is no shift or distortion of the characteristic peak after the P(S-*b*-MMA) modification (π - π stacking or coordination). The similar Raman patterns indicate that the overall BN structure is preserved after surface modification with few, if any, defects.

[1] A. Pakdel, C. Zhi, Y. Bando, T. Nakayama and D. Golberg, *ACS Nano*, 2011, **5**, 6507.

*S7. Characterization of SM-*pi*-BNNSs solubility*



Fig. S9. Digital image of SM-*pi*-BNNSs redispersed in cyclohexane, acetone and toluene (from left to right). All the samples were kept for 48 h before photographing. The concentrations of SM-*pi*-BNNSs in acetone and toluene are ~ 78 and 123 mg L^{-1} separately as determined by Beer-Lambert plotting at 300 nm [1].

[1] N. Chen, Y.-T. Liu, X.-M. Xie, X.-Y. Ye, X. Feng, Y.-F. Chen and Y.-H. Wang, *Carbon*, 2012, **50**, 4760.

S8. HRTEM images of SM-*pi*-BNNs and SM-*co*-BNNs

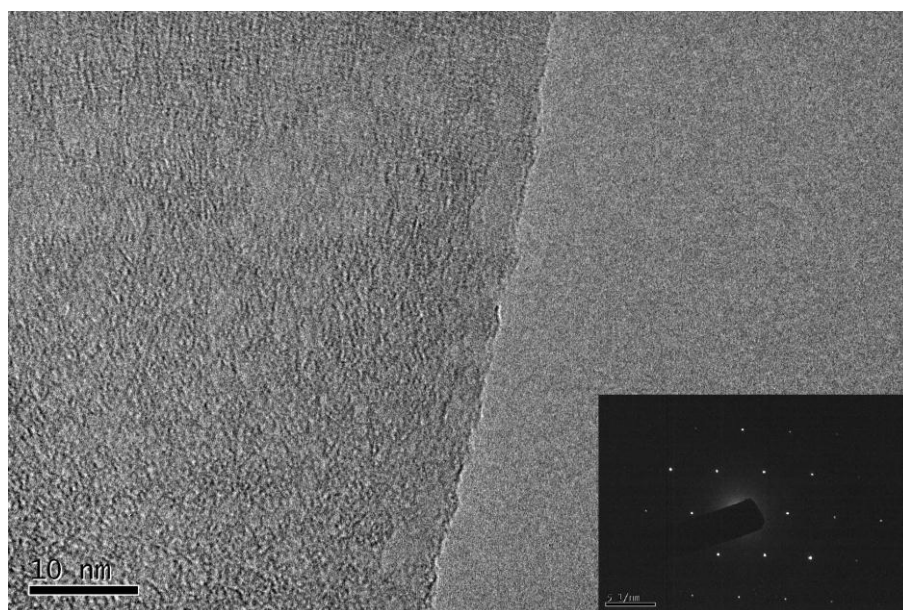


Fig. S10. HRTEM image of an SM-*pi*-BNNs from acetone and the corresponding ED pattern (insert).

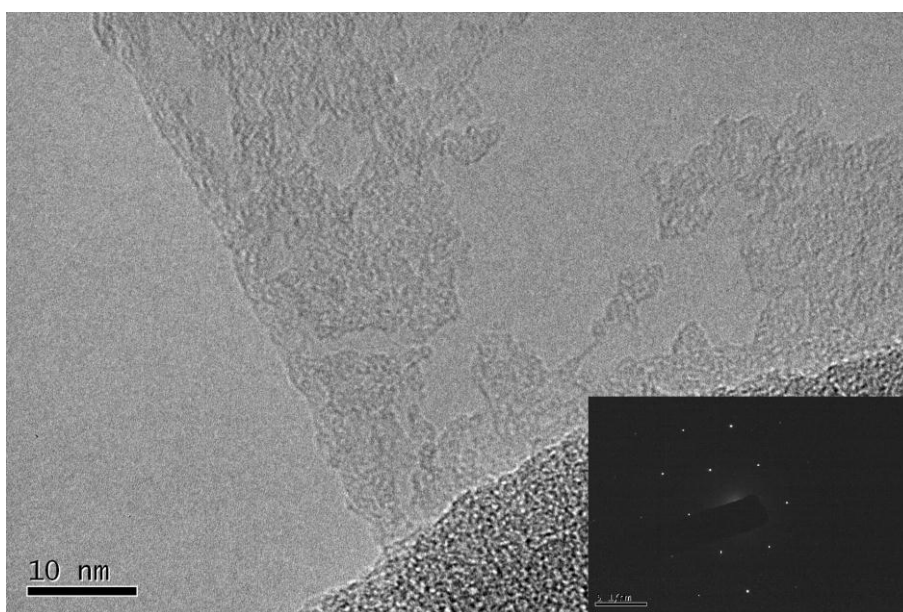


Fig. S11. HRTEM image of an SM-*co*-BNNs from cyclohexane and the corresponding ED pattern (insert).

S9. Digital images of nanocomposite films



Fig. S12. Digital image of an SM-*pi*-BNNSs/PMMA nanocomposite film.

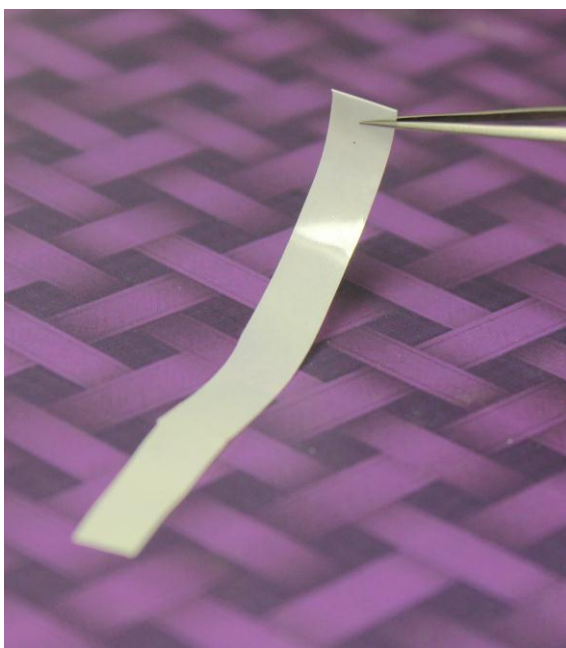


Fig. S13. Digital image of an SM-*co*-BNNSs/PS nanocomposite film.

S10. Representative S-S curves of nanocomposite films

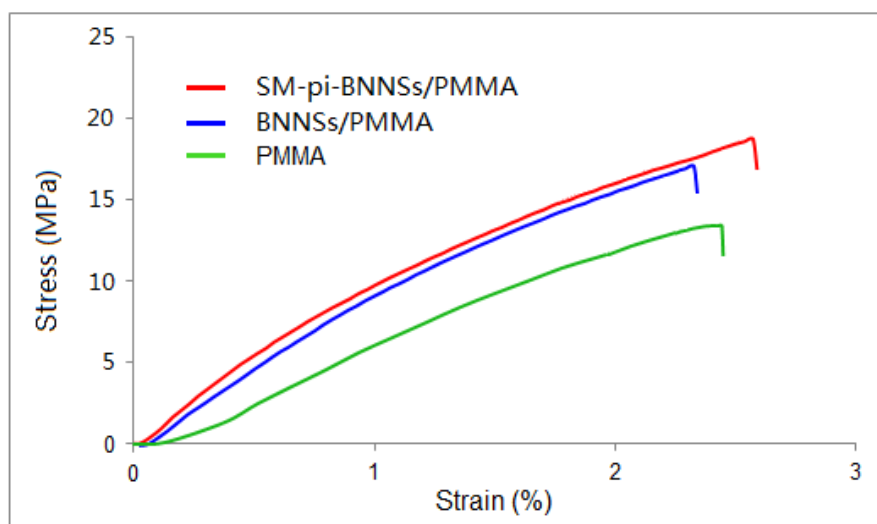


Fig. S14. Representative S-S curves of PMMA, BNNSs/PMMA and SM-*pi*-BNNSs/PMMA films.

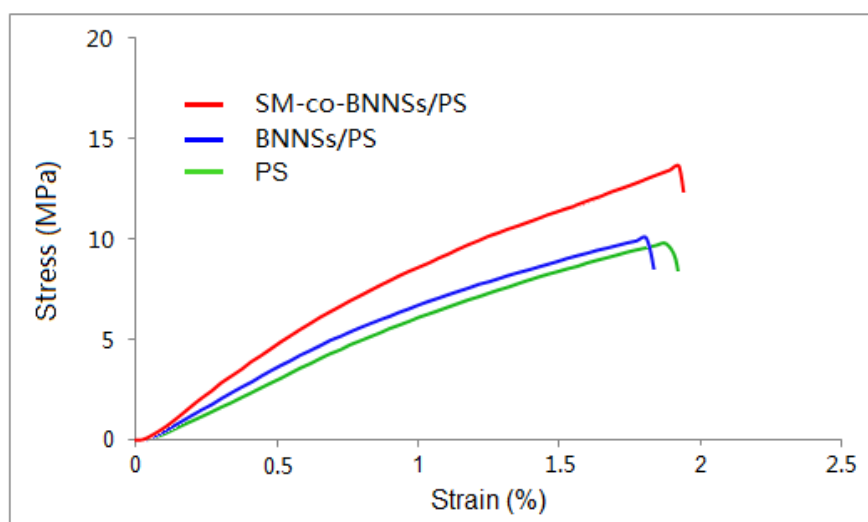
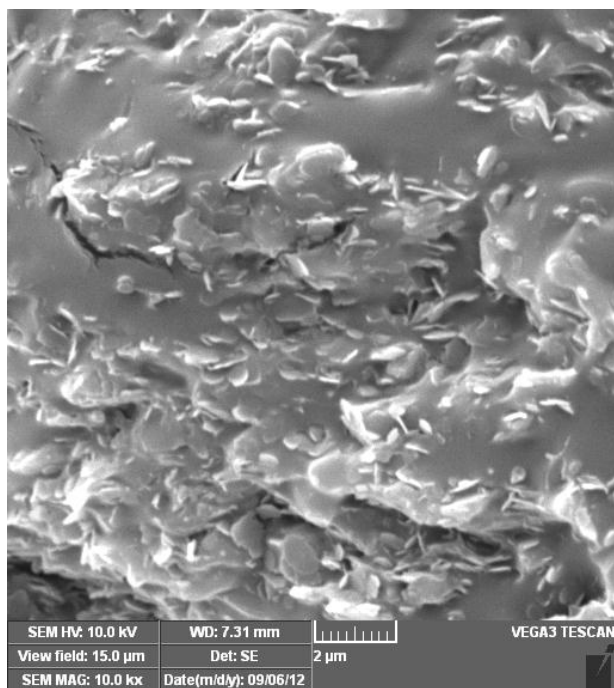
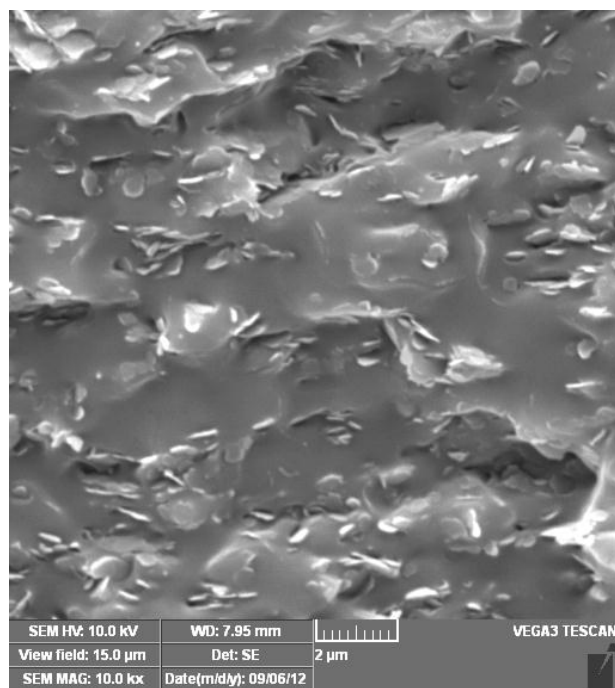


Fig. S15. Representative S-S curves of PS, BNNSs/PS and SM-*co*-BNNSs/PS films.

S11. SEM images of nanocomposite films

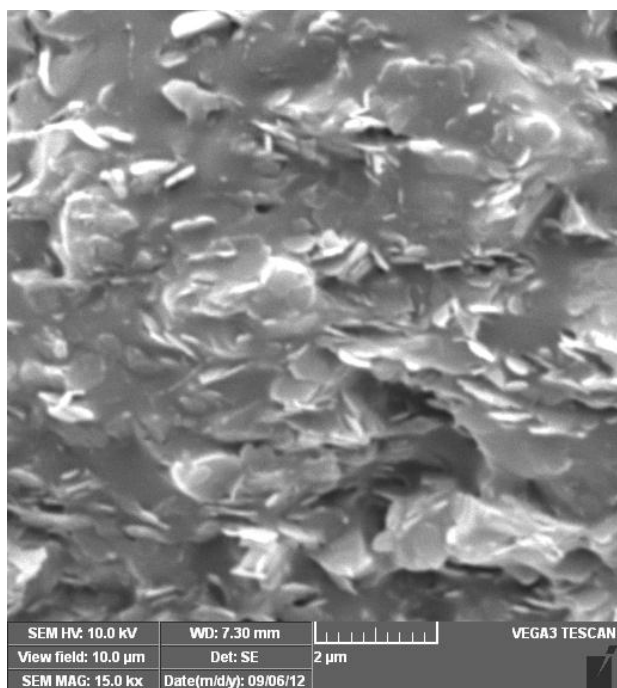


(a)

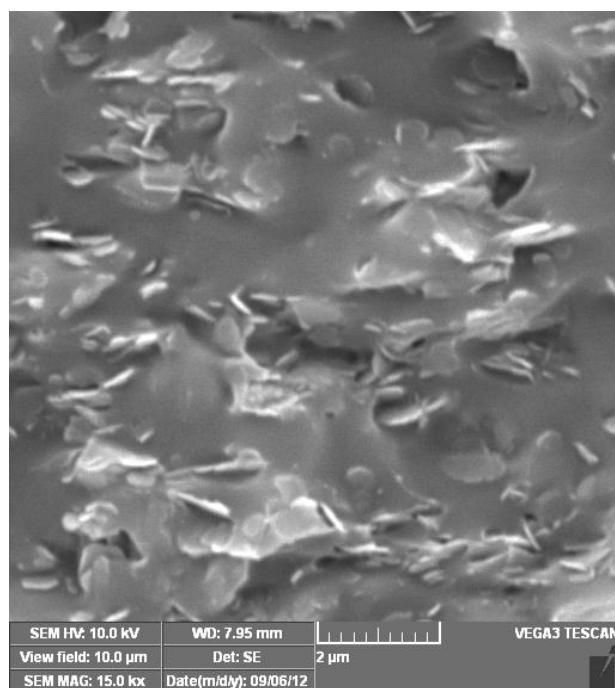


(b)

Fig. S16. Cross-sectional SEM images of (a) BNNSs/PMMA and (b) SM-*pi*-BNNSs/PMMA films.



(a)



(b)

Fig. S17. Cross-sectional SEM images of (a) BNNSs/PS and (b) SM-*co*-BNNSs/PS films.